

Anode Catalysts for Direct Hydrazine Fuel Cells: From Laboratory Test to an Electric Vehicle

Alexey Serov, Monica Padilla, Aaron J. Roy, Plamen Atanassov,* Tomokazu Sakamoto, Koichiro Asazawa, and Hirohisa Tanaka

Abstract: Novel highly active electrocatalysts for hydrazine hydrate fuel cell application were developed, synthesized and integrated into an operation vehicle prototype. The materials show in both rotating disc electrode (RDE) and membrane electrode assembly (MEA) tests the world highest activity with peak current density of $16\,000\text{ A g}^{-1}$ (RDE) and 450 mW cm^{-2} operated in air (MEA).

The automotive world will be changed in 2015, when leading manufacturers will publicly introduce their first generation of commercial fuel cell vehicles. It should be noticed, however, that these automobiles were developed with proton exchange membrane (PEM) technology and membrane electrode assemblies (MEAs) in fuel stacks containing platinum catalysts for both hydrogen oxidation and oxygen reduction.

There are several drawbacks of PEM-based technology, including: the high cost of fuel cell membranes, the extremely high cost of platinum, and the absence of a developed hydrogen infrastructure. Further, the use of hydrogen requires a high-pressure tank, which requires a full redesign of the automobile frame. These factors result in a high-cost commercial vehicle with a low driving range and safety issues.

In contrast to PEM hydrogen fueled vehicles development, researchers from Daihatsu Motor Co. have introduced the idea of anion-exchange membrane fuel cell with liquid fuels.^[1–11] Switching from acidic proton exchange to alkaline, anion-exchange membranes has many benefits, including: 1) fast fuel oxidation and oxygen reduction and 2) possible use of cheaper non-platinum group metal catalysts as anode and cathode material for both sides of the MEA. The liquid fuel of choice was hydrazine hydrate, which has no carbon atoms and thus will not contribute to increased CO_2 levels, the theoretical electromotive force is 1.56 V and it can be oxidized by number of cheap catalysts.^[12] To meet the power output requirements of a stack with limited size, the anode material should provide the highest power density, be stable, and selective toward the production of water and nitrogen with no ammonia (NH_3) generation. Up to now, catalysts reported

had a low activity with operation in air (real vehicles operation conditions).

Herein we report the synthesis of novel Ni-based supported catalysts by a completely solvent-free method. The method is based on a mechanochemical approach and is scalable to hundreds of kilograms of catalyst and can be considered a “green” synthesis method compared with conventional synthesis, which requires the use of solvents. These catalysts show high activity in both rotating disc electrode (RDE) and MEA tests, with real vehicles operation conditions. The effects of catalysts loading and carbon addition on hydrazine electrooxidation were studied on nickel-based materials for the first time.

These electrocatalysts for hydrazine electrooxidation were synthesized by solvent-free impregnation of nickel and zinc precursors by using a high-energy mechanochemical approach. The synthesized materials were comprehensively characterized by Brunauer–Emmett–Teller (BET) method, scanning electron microscopy (SEM), transmission electron microscopy (TEM), and X-ray diffraction (XRD); their electrochemical activity was measured by RDE and fuel cell tests.

X-ray diffraction patterns for the NiZn catalysts are shown in Figure 1. Analysis revealed that all three catalysts consist of mainly $\text{Ni}_{87}\text{Zn}_{13}$ phase (abbreviated here as NiZn). A minor phase, identified as ZnO, was detected in the NiZn catalysts, resulting in various NiZn:ZnO ratios in the overall bulk composition: 85:15, 85:15, and 95:5 (20 wt %, 40 wt %, and 60 wt %).

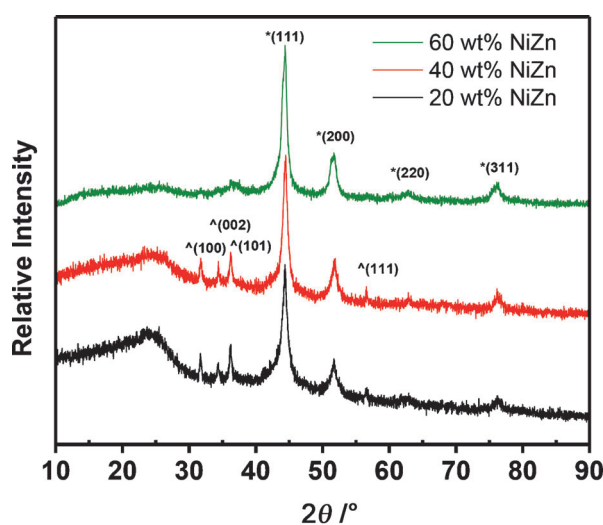


Figure 1. XRD data for NiZn catalysts with different loading synthesized by a mechanochemical method.

[*] Dr. A. Serov, M. Padilla, A. J. Roy, Prof. Dr. P. Atanassov
Chemical & Nuclear Engineering Department, UNM Center for
Emerging Energy Technologies, University of New Mexico
Albuquerque, NM 87131 (USA)
E-mail: plamen@unm.edu

T. Sakamoto, Dr. K. Asazawa, Dr. H. Tanaka
Frontier technology R & D Division, Daihatsu Motor Co., Ltd.
Ryuo, Gamo, Shiga 520-2593 (Japan)



Supporting information for this article is available on the WWW
under <http://dx.doi.org/10.1002/ange.201404734>.

and 60 wt %, respectively). The presence of zinc oxide in the catalysts can be explained by the extremely high oxophilicity of Zn metal. We observed that even controlled passivation of the reduced samples could not prevent oxide formation upon exposure to air. However, operation of the catalysts in the highly reductive environment of 20 wt % of hydrazine hydrate (HH) will lead to ZnO reduction. MEAs post-mortem analysis is required in order to confirm this hypothesis. Calculation of the particle grain size by Scherrer analysis of the refined patterns gave an average particle domain size for all catalyst in the range of 10–15 nm, which was confirmed by particle size distribution from TEM images (see Figure S1 in the Supporting Information).

Morphological analysis by SEM and particles distribution on support by TEM is shown in Figure 2 A–C and Figure 2 D–F, respectively. SEM images revealed that catalysts preserved a morphology typical for materials synthesized on high surface area Ketjenblack carbons (Figure 2 A–C). From the TEM images it is observed that catalysts with 40 wt % and 60 wt % are evenly coated on the support surface without significant agglomeration. In the case of low loaded material with 20 wt % of NiZn the surface was not fully covered, due to a high carbon-to-catalyst ratio (Figure 2 D–E). However, it was also confirmed that the catalyst is not agglomerated (Figure 2 D).

Previously our group has implemented a spray pyrolysis method for synthesis of unsupported NiZn electrocatalysts.^[5] Figure 3 compares the electrochemical performance of the supported catalysts with spray-pyrolyzed nickel-based materials. It can be seen in Figure 3 that the supported catalysts possess higher overall mass activity and improved onset

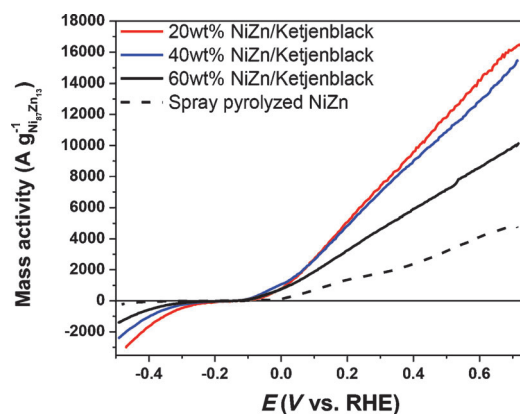


Figure 3. Cyclic voltammograms of NiZn catalysts with different metal loading compared to unsupported spray-pyrolyzed NiZn. Conditions: catalyst total loading 20 μg , 1 M KOH, 5 wt % hydrazine hydrate, 60 °C, N_2 purge, 1600 r.p.m.

potential (ca. -0.14 V vs. RHE) compared to unsupported NiZn. Considering that the particle size for unsupported NiZn was in the range of 20–60 nm, the higher electrochemical activity of the NiZn/KB catalysts directly confirms the existence of a pore size distribution (PSD) effect. It is found that the 20 wt % and 40 wt % NiZn/KB catalysts have similar onset potentials and a peak activity of ca. $16000 \text{ A g}_{\text{NiZn}}^{-1}$, to our knowledge the highest mass activity of electrocatalysts for HH oxidation published.

The mechanism of HH oxidation on unsupported catalysts was previously hypothesized from in situ infrared adsorption spectroscopy (IRRAS) experiments.^[5] These same experiments were performed with our supported catalysts and confirmed that the observed mechanism is not visibly altered by the inclusion of carbon and a different synthesis method. Figure 4 shows the appearance and disappearance of species critical to the reaction mechanism. Notable is a decreased signal from N–H/O–H (3225 cm^{-1}) indicating species consumption and increased signals from $-\text{NH}_2^{2+}$ (2775 cm^{-1}), Ni–

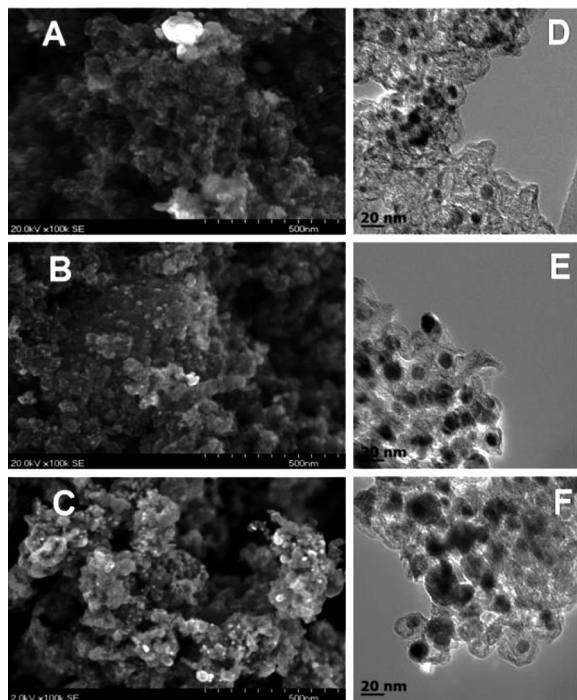


Figure 2. SEM (left) and TEM (right) images of $\text{Ni}_{87}\text{Zn}_{13}/\text{KB}$ prepared by ball-milling with different loadings: 20 wt % (A and D), 40 wt % (B and E), and 60 wt % (C and F).

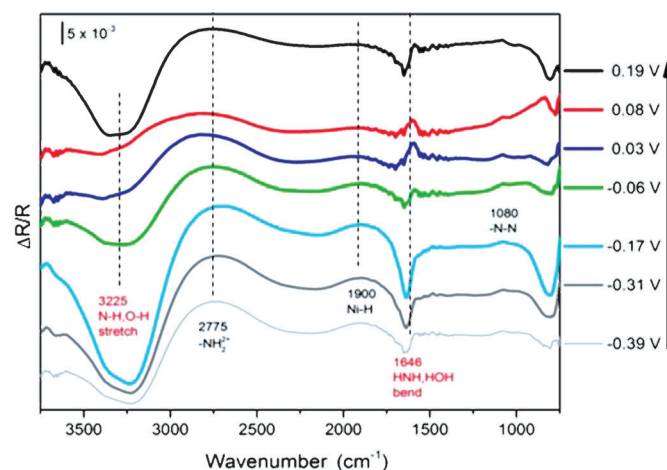


Figure 4. In situ IRRAS with simultaneous linear voltammetry. 60 wt % NiZn, 1 M KOH + 5 wt % HH, room temperature, no rotation, $76.5 \mu\text{g cm}^{-2}$ catalyst, 1 mV s^{-1} , V vs. reversible hydrogen electrode (RHE).

H (1900 cm^{-1}), and HNH/HOH (1646 cm^{-1}) indicating the presence of intermediate oxidation species. The presence of N–N (1080 cm^{-1}), which is characteristic of HH, is also noted. These same trends (increasing/decreasing signals) were observed for unsupported catalysts, suggesting that the reaction pathway is the same for supported catalysts synthesized by mechanochemical methods.

To confirm the high activity of the supported NiZn/KB catalysts, single-cell MEA tests were performed with a Fe-aminoantipyrine-derived catalyst as cathode material synthesized by a sacrificial support method (SSM).^[13–23] Despite the fact the in RDE experiments 20 wt % NiZn/KB had a slightly higher peak activity with respect to MEA building, the 60 wt % catalyst was selected for fuel cell testing. The low density of 20 wt % NiZn/KB results in a significantly thicker catalyst layer with poorly developed triple-phase boundary. Figure 5 compares the activities of a supported and an unsupported NiZn catalyst.

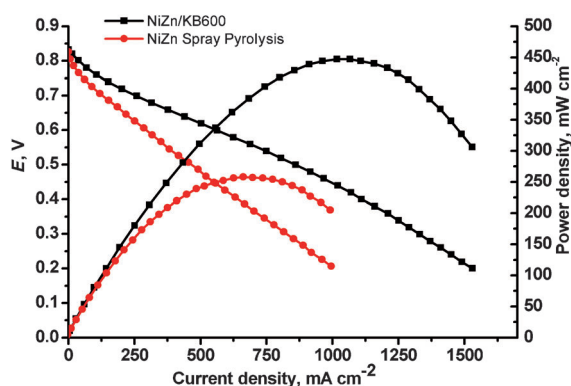


Figure 5. MEA performance of two different NiZn materials. Conditions: catalyst loading 2 mg cm^{-2} (anode), 1 mg cm^{-2} (cathode); $T_{\text{cell}} = 80^\circ\text{C}$, HH flow rate = 2 mL min^{-1} (20 wt %), air flow rate = 500 cm^3 .

It is clear that a two-fold increase of activity in peak current density can be achieved by using carbon supports. The higher performance of NiZn/KB vs. NiZn in RDE tests can be explained by the particle size effect. However, in MEA tests the situation is more complex. Factors to consider include possible mass transfer limitations of HH to the active sites of the catalyst, the removal of gases from the catalytic layer, and possible interactions between ionomer and catalyst. Additionally, the unsupported catalyst has a surface area one order of magnitude less than NiZn/KB. The increase of surface area in supported materials results in an increased retention time of HH in contact with the active sites of the catalyst, resulting in an increase of power density.^[24–] It should be noted that peak current density for 60 wt % NiZn/KB of 450 mW cm^{-2} (HH/air) is the highest ever reported.

Reported here is the world's highest activity of Ni-based supported electrocatalysts, which meets Daihatsu Co.'s performance criteria. This material has been implemented in a fuel stack for a new generation of an HH-fueled vehicle, which was designed, built, and presented in 2013 at the 43rd Tokyo Motor Show (Figure 6).

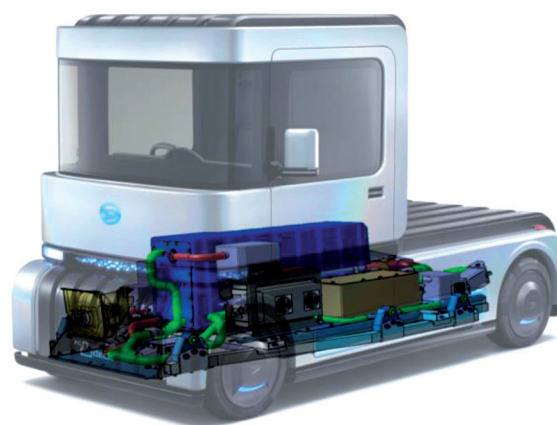


Figure 6. Daihatsu fuel cell electric vehicle with an alkaline membrane fuel cell stack (blue) using hydrazine hydrate as fuel. The vehicle was presented at the Tokyo Motor Show in December 2013.

In conclusion, a novel family of supported electrocatalysts based on NiZn material was designed and synthesized by a solvent-free environmentally benign method. The materials were found to be nanosized with a fine particle distribution on the carbon support. The absence of agglomeration results in high catalyst utilization with peak current density of 16000 A g^{-1} . MEAs were designed and tested by Daihatsu Motor Co., and for the first time, an activity with air higher than 450 mW cm^{-2} was measured.

Received: April 28, 2014

Revised: June 7, 2014

Published online: August 12, 2014

Keywords: fuel cells · hydrazine hydrate · membrane electrode assembly · nickel · supported catalysts

- [1] T. Sakamoto, P. Deevanhxay, K. Asazawa, S. Tsushima, S. Hirai, H. Tanaka, *J. Power Sources* **2014**, 252, 35–42.
- [2] T. Sakamoto, K. Asazawa, J. Sanabria-Chinchilla, U. Martinez, B. Halevi, P. Atanassov, P. Strasser, H. Tanaka, *J. Power Sources* **2014**, 247, 605–611.
- [3] T. Sakamoto, K. Asazawa, U. Martinez, B. Halevi, T. Suzuki, S. Arai, D. Matsumura, Y. B. Nishihata, P. Atanassov, H. Tanaka, *J. Power Sources* **2013**, 234, 605–611.
- [4] S.-I. Yamazaki, Z. Siroma, N. Fujiwara, M. Asahi, K. Asazawa, H. Tanaka, T. Ioroi, *Electrochim. Acta* **2013**, 94, 38–41.
- [5] U. Martinez, K. Asazawa, B. Halevi, A. Falase, B. Kiefer, A. Serov, M. Padilla, T. Olson, A. Datye, H. Tanaka, P. Atanassov, *Phys. Chem. Chem. Phys.* **2012**, 14, 5512–5517.
- [6] J. Sanabria-Chinchilla, K. Asazawa, T. Sakamoto, S. Yamaguchi, K. Yamada, H. Tanaka, P. Strasser, *J. Am. Chem. Soc.* **2011**, 133, 5425–5431.
- [7] K. Asazawa, T. Sakamoto, S. Yamaguchi, K. Yamada, H. Fujikawa, H. Tanaka, K. Oguro, *J. Electrochem. Soc.* **2009**, 156, B509–B512.
- [8] K. Asazawa, K. Yamada, H. Tanaka, A. Oka, M. Taniguchi, T. Kobayashi, *Angew. Chem.* **2007**, 119, 8170–8173; *Angew. Chem. Int. Ed.* **2007**, 46, 8024–8027.
- [9] K. Yamada, K. Yasuda, T. Ioroi, N. Fujiwara, Z. Siroma, H. Tanaka, Y. Miyazaki, T. Kobayashi, *Electrochem. Commun.* **2003**, 5, 892–896.

- [10] K. Yamada, K. Yasuda, T. Ioroi, H. Tanaka, Y. Miyazaki, T. Kobayashi, *J. Power Sources* **2003**, *122*, 132–137.
- [11] K. Yamada, K. Asazawa, K. Yasuda, T. Ioroi, H. Tanaka, Y. Miyazaki, T. Kobayashi, *J. Power Sources* **2003**, *115*, 236–242.
- [12] A. Serov, C. Kwak, *Appl. Catal. B* **2010**, *98*, 1–9.
- [13] A. Serov, U. Martinez, A. Falase, P. Atanassov, *Electrochem. Commun.* **2012**, *22*, 193–196.
- [14] S. Pylypenko, S. Mukherjee, T. S. Olson, P. Atanassov, *Electrochim. Acta* **2008**, *53*, 7875–7883.
- [15] M. H. Robson, A. Serov, K. Artyushkova, P. Atanassov, *Electrochim. Acta* **2013**, *90*, 656–665.
- [16] S. Brocato, A. Serov, P. Atanassov, *Electrochim. Acta* **2013**, *87*, 361–365.
- [17] A. Serov, M. H. Robson, K. Artyushkova, P. Atanassov, *Appl. Catal. B* **2012**, *127*, 300–306.
- [18] A. Serov, M. H. Robson, M. Smolnik, P. Atanassov, *Electrochim. Acta* **2012**, *80*, 213–218.
- [19] A. Serov, M. H. Robson, B. Halevi, K. Artyushkova, P. Atanassov, *Electrochem. Commun.* **2012**, *22*, 53–56.
- [20] A. Falase, M. Main, K. Garcia, A. Serov, C. Lau, P. Atanassov, *Electrochim. Acta* **2012**, *66*, 295–301.
- [21] A. Serov, U. Martinez, P. Atanassov, *Electrochem. Commun.* **2013**, *34*, 185–188.
- [22] A. Serov, M. H. Robson, M. Smolnick, P. Atanassov, *Electrochim. Acta* **2013**, *109*, 433–439.
- [23] A. Serov, A. Aziznia, P. H. Benhangi, K. Artyushkova, P. Atanassov, E. Gyenge, *J. Mater. Chem. A* **2013**, *1*, 14384–14391.
- [24] A. Serov, K. Artyushkova, P. Atanassov, *Adv. Energy Mater.* **2014**, DOI: 10.1002/aenm.201301735.
- [25] P. S. Ruvinskiy, A. Bonnefont, C. Pham-Huu, E. R. Savinova, *Langmuir* **2011**, *27*, 9018.
- [26] P. S. Ruvinskiy, A. Bonnefont, M. Bayati, E. R. Savinova, *Phys. Chem. Chem. Phys.* **2010**, *12*, 15207.
- [27] A. Schneider, L. Colmenares, Y. E. Seidel, Z. Jusys, B. Wickman, B. Kasemo, R. J. Behm, *Phys. Chem. Chem. Phys.* **2008**, *10*, 1931.
- [28] P.-Y. Olu, C. Barros, N. Job, M. Chatenet, *Electrocatalysis* **2014**, *5*, 288–300.
- [29] K. S. Freitas, B. M. Concha, E. A. Ticianelli, M. Chatenet, *Catal. Today* **2011**, *170*, 110.